RESEARCH ARTICLE

3D QSAR Analysis of Flavones as Antidiabetic agents

Navin Sainy[1], Nidhi Dubey[1] , Rajesh Sharma[1], Nitin Dubey[2], Jitendra Sainy[1]
School of Pharmacy, Devi Ahilya Vishwavidyalaya, Indore (M.P.) 452001, India.
[2]College of Pharmacy, IPS Academy Indore (M.P.) 452012, India.
*Corresponding Author E-mail: **nsainy23@gmail.com**

ABSTRACT:
Diabetes is the most prevailing disease worldwide and emerged as the fourth leading cause of mortality. Inhibition of intestinal α-Glucosidase enzyme is an effective approach for controlling post prandial hyperglycemia. α-Glucosidase inhibitors are known to be very effective in decreasing post-prandial hyperglycemia but the existing drugs are weak inhibitors of α-Glucosidase and also have side effects. Hence it needs for new therapeutic candidate which can effectively inhibit the activity of α-Glucosidase. Flavones recognized as the potential lead structure for many pharmacological activities. In the present research work 3D QSAR (comparative molecular field analysis and comparative molecular similarity indices analysis) was carried out on a series of flavones to identify structural requirement for effective inhibition of α-Glucosidase enzyme. The QSAR results shows that the LOO cross-validated q^2 values of CoMFA and CoMSIA models are 0.742 and 0.759, respectively. The outcome of this research work could be effectively utilized for design of better α-Glucosidase inhibitors.

KEYWORDS: α-Glucosidase, Flavone, CoMFA, CoMSIA.

INTRODUCTION:
Diabetes mellitus (DM) is one of the most prevalent metabolic diseases in the world causes due to defects in insulin secretion and action. This is due to the increase of level of glucose in the blood (hyperglycemia) and causes impairment of functioning to important organs like blood vessels and nerves. It remains fourth leading cause of death among all the existing non-communicable diseases and study showed that the figure of diabetes mellitus patients increases every year. According to World Health Organization report 2020, In 2014, worldwide 8.5% of people of age 18 years and older living diabetes. International Diabetes Federation estimated that there are 415 million people living with diabetes, possibly will reach up to 642 million in 2040.Among these, 80% of people live in low and middle-income countries.[1] The availability of treatment for both Type-1 and Type-2 diabetes is either limited or the development of resistance and toxicity is causing serious concern in this field.[2]

Therefore, the discovery of novel effective therapeutic agents for diabetes with minimum side effects and toxicity is essentially important. Type-2 diabetes mellitus can be efficiently managed by inhibiting the absorption of carbohydrates after a meal, thus controlling the post-prandial hyperglycemia, α-Glucosidase is a characteristic exo-type glycosidase enzyme that catalyzes the liberation of α-glucosides from the non-reducing end of the carbohydrates.[3] It is the key enzyme involved in intestinal glucose absorption.

In DM hyperglycemia can leads to chronic dysfunctions of various organ system.[4,5] Hence, management of blood glucose level is an important approach to decrease diabetes related disorders. Recently, the α-glucosidase inhibitors have gained immense pharmaceutical interest due to their abilities to effectively reduce the dietary carbohydrate uptake and suppress postprandial hyperglycemic condition. Hence, the α-glucosidase inhibitors remain superior therapy for type-2 diabetes[6]. Most of the α-glucosidase inhibitors developed till date namely acarbose, voglibose, and miglitol are widely used oral drugs since the early 1990s for the treatment of type-2 diabetes. Though they cause various side effects, such as flatulence, diarrhea and abdominal discomfort.[8]

They all three also have low efficacy against enzymes with high IC_{50} values[9]. Owing to the vital role of this enzyme in hyperglycemia and side effects of the existing drugs, the discovery of non-carbohydrate based small organic molecules as α-glucosidase inhibitors would be of greatest help in finding a pharmacokinetically valuable molecule for diabetes. Huge amount of literature is mounting in support of natural products such as polyphenolic compounds, flavonoids, flavanols, and terpenoids as α-glucosidase inhibitors. Finding a synthetic equivalent to above natural products will provide a bioavailable lead compound. Flavone is an important scaffold present in various pharmacologically active compounds. They possess structural diversity and different biological activity[10-17]. Because of this reason the attention of researchers has been increasing to further study flavones as lead compounds to cure several diseases. Various studies revealed that flavonoids could decrease hyperglycemia, increase sensitivity and improve the secretion of insulin[13], hence flavones could be utilized as lead structure for further drug discovery.

Now a days Quantitative Structure Activity relationship (QSAR) analysis and other computational techniques have been most popular in designing new drugs[18-24]. In present research work we have been employed comparative molecular field analysis (CoMFA) and comparative molecular similarity indices analysis (CoMSIA)[25-29] methodologies for investigating structural constraint in the vicinity of flavones which may be useful in designing new flavones class of anti-diabetic drug.
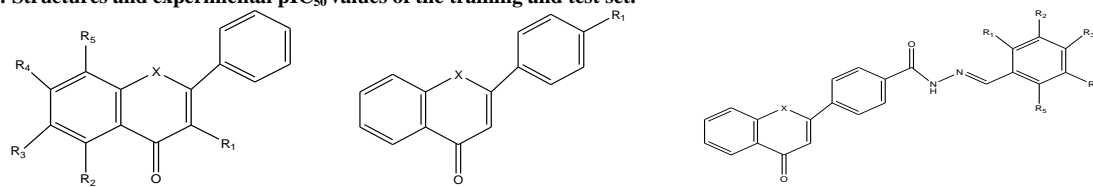
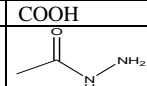## MATERIALS AND METHODS:
Materials:
SYBYL-X 2.1 software was used to perform comparative molecular field analysis (CoMFA), and comparative molecular similarity indices analysis (CoMSIA)

Data set:
The data set composed of forty-one flavone derivatives possessing anti-diabetic activity[30,31]. were utilized to develop 3D QSAR models. The IC_{50} values i.e., the concentration (μM) of compound that gives 50% inhibition were changed into pIC_{50} (-log IC_{50}) values and utilized as a dependent variable in CoMFA and CoMSIA analysis. Forty-one flavone derivatives were randomly segregated into the training set (27 compounds) and test sets (14 compounds). The test compounds were chosen on the basis of structural diversity and broad range of activity within data set. Chemical structures of flavones derivatives and their biological activities are showed in Table **1**.

Table 1: Structures and experimental pIC$_{50}$ values of the training and test set.

01-09　　　　**10-11**　　　　**12-42**

| Comp.	R$_1$	R$_2$	R$_3$	R$_4$	R$_5$	X	pIC$_{50}$	Comp.	R$_1$	R$_2$	R$_3$	R$_4$	R$_5$	X	pIC$_{50}$
01	H	OH	OH	OH	H	O	4.2839	23*	H	OCH$_3$	H	OCH$_3$	H	O	3.2055
02	H	OH	OH	OH	H	NH	4.3467	24	Br	H	OH	H	H	O	3.2310
03*	H	OH	OH	OH	H	O	4.1023	25	Me	H	H	H	H	O	3.3121
04	OH	OH	OH	OH	H	O	3.8153	26	H	Me	H	H	H	O	3.3032
05*	Ben	OH	OH	OH	H	O	3.1938	27	H	H	Me	H	H	O	3.4348
06	Hydroxybenzene	OH	OH	OH	H	O	3.2048	28	Cl	H	H	H	H	O	4.5287
07	**H**	**OH**	**H$_2$N**	**OH**	**H**	**O**	**5.6197**	29	H	Cl	H	H	H	O	4.1904
08	H	H	H$_2$N	OH	H	O	3.8696	30*	H	H	Cl	H	H	O	4.4168
09*	H	OH	H$_2$N	OH	NH$_2$	O	4.0861	31	NO$_2$	H	H	H	H	O	3.9086
10	COOH	H	H	H	H	O	3.0958	32*	H	NO$_2$	H	H	H	O	4.0087
11*	(structure)	H	H	H	H	O	3.1366	33	H	H	NO$_2$	H	H	O	4.0535
12	OH	H	OH	H	OH	O	4.8124	34	fl	H	H	H	H	O	4.7670
13*	OH	OH	H	H	H	O	4.7721	35	H	fl	H	H	H	O	4.6420
14*	OH	H	OH	H	H	O	4.5638	36	H	H	fl	H	H	O	4.7121
15	OH	H	H	OH	H	O	4.4225	37	H	OCH$_3$	H	H	H	O	3.1671
16*	H	OH	OH	H	H	O	4.7644	38	H	H	OCH$_3$	H	H	O	3.1609
17*	OH	H	H	H	H	O	4.4271	39	Pyr	H	H	H	H	O	3.3121
18	H	OH	H	H	H	O	4.0639	40	H	Pyr	H	H	H	O	3.2834
19	H	H	OH	H	H	O	4.5622	41	H	H	Pyr	H	H	O	3.3663
20*	OH	H	OCH$_3$	H	H	O	4.5316								
21*	H	OH	OCH$_3$	H	H	O	4.4634								

*Test set

Molecular modeling:
The three-dimensional (3D) structure of flavones were constructed by means of sketch module of the SYBYL-X 2.1 and the energy is minimized by MMFF94 (Merck molecular force field 94) and then the addition of Gasteiger–Huckle charge iscarried out by SYBYL-X 2.1.

Molecular alignment for CoMFA and CoMSIA analysis:
It is observed that molecular alignment is one of the most significant and subtle parameters in 3D-QSAR. To develop reliable 3D-QSAR models, the CoMFA and CoMSIA techniques need appropriate alignment of compounds[32]. For aligning all the compounds of data set maximum common substructure technique was employed. The most active compound 07 (IC50=1.0 μM, pIC50 = 5.697) of dataset was set as template for aligning test and training set compounds. The DATABASE ALIGN option of SYBYL-X 2.1 was used to align all the compounds above template molecule by rotation and translation so as to minimize the RMSD between atoms in the template and the corresponding atoms in the analogues. The template compound **07** with maximum common substructure (bold stick) and aligned molecules are shown in figure 1.

(a)
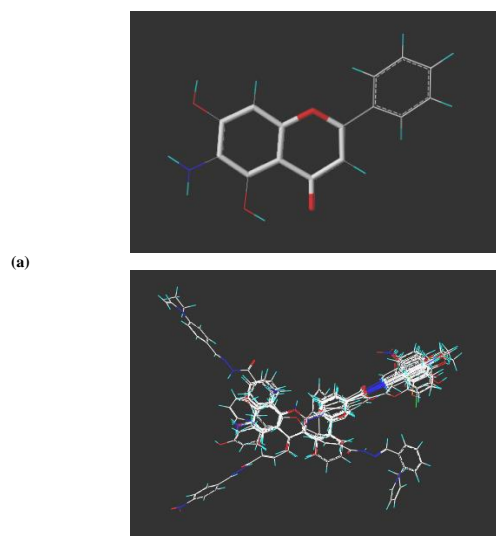
(b)

Figure 1: (a) Structure of most active compound 07 (template) and maximum common substructure in bold stick; (b) molecular alignment of all molecules over template molecule

Calculation of comparative molecular field analysis descriptors:
The CoMFA and CoMSIA models were analyzed through SYBYL-X 2.1 molecular modeling software[28]. For CoMFA calculations, steric and electrostatic interactions were calculated through an sp^3 hybridized carbon atom with a Van der Waals radius of 1.52Å and a +1 charge as steric and electrostatic probes, respectively,

and Tripos force field with a distance-dependent dielectric constant at all intersections in a regularly spaced grid (2 Å).The maximum steric and electrostatic energy cut off was taken as 30kcal/mol. The lowest column filtering was set to 2.0kcal/mol to enhance the signal-to-noise ratio by neglecting those lattice points whose energy difference was lower than this threshold.

Calculation of comparative molecular Similarity indices analysis descriptors:
Five CoMSIA similarity index fields (steric, electrostatic, hydrophobic, H-bond donor and H-bond acceptor) were evaluated using the sp^3 hybridized carbon probe atom with a radius of 1 Å and a +1 charge placed at the lattice points of the same area of grid as it was used for the CoMFA calculations. A distance-dependent Gaussian type was employed between the grid point and each atom of the molecule. The default value of 0.3 was employed as the attenuation factor. The least column filtering was set to 1.0kcal/mol.

Partial least square analysis:
The regression analysis was performed by means of the partial least square analysis method[33-41]. The cross-validation analysis was accomplished by the LOO technique, wherein one compound is taken out from the dataset and its activity is predicted through the model developed from the rest of the data set.A final non-cross-validated analysis was carried in sequence with the optimal number of components received from the LOO method and was then utilized to evaluate the results.The cross-validated correlation coefficient (q^2) that bring out the optimum number of components and lowest SEE was take in to consideration for further analysis and calculated using the following formula.

$$q^2 = \frac{\Sigma(\gamma_{pred} - \gamma_{pred})^2}{\Sigma(\gamma_{actual} - \gamma_{mean})^2}$$

where, γ_{pred}, γ_{actual} and γ_{mean} are predicted, actual, and mean values of the target property (pIC$_{50}$) respectively. Equal weights for CoMFA were given to steric and electrostatic fields using CoMFA_STD scaling option. To develop 3D-QSAR models CoMFA and CoMSIA descriptors were utilized as an independent variable and pIC$_{50}$ activity value as dependent variable.

Predictive correlation coefficient:
The predictive capability of developed QSAR models were validated by means of a test set of fourteen compounds that were leave out during model generation. The energy minimization and geometry optimization of these fourteen molecules is similar as that of the training set compounds explained above, and their activity was calculated utilizing the model obtained from the training

set. The predictive coefficient of determination (r^2pred), which is based on the test set molecules, is calculated using the formula.[35]

$$r^2_{pred} = \frac{(SD - PRESS)}{SD}$$

where SD is the sum of the squared deviation between the biological activity of the test setmolecules and the mean activity of the training set molecules. Predictive residual sum of square (PRESS) is computed by taking the difference in predicted and actual activity of the test set molecules. For all conventional analysis (non-cross-validation) the 'minimum sigma' standard deviation threshold was set to 2.0kcal/mol.

RESULTS:
CoMFA analyses:
The steric and electrostatic CoMFA fields produced a cross-validated $q^2 = 0.742$ with six components, non-cross-validated r^2 of 0.923, SEE = 0.154 and F value of 36.36. The contribution of the steric and electrostatic fields is 70.30% and 29.70%, respectively.

CoMSIA analyses:
Overall, twelve CoMSIA models were developed through various combinations of molecular fields. Models together with the combination of steric, hydrophobic, hydrogen-bond donor and acceptor fields produced the highest q^2 (0.759) with six components, and r^2 (0.961) with a SEE of 0.105. The contributions of steric, electrostatic, hydrophobic, hydrogen-bond donor and acceptor fields were 22.50%, 17.90%, 20.10%, 17.30% and 22.20%, respectively. The statistical parameters for CoMSIA and CoMFA are presented in Tables 2 and 3.

Validation of QSAR models:
The predictive ability of the CoMFA (r^2pred = 0.901) and CoMSIA (r^2 pred = 0.900) models were found acceptable and the results are shown in Table 3. results confirmed the robustness of generated QSAR model, and it expressed good conformity between the experimental and predicted pIC_{50} values (Table 4). The plots of predicted versus actual activity values for training and test set molecules for CoMFA and CoMSIA are shown in figure 2(a) and (b).

Table 2: Summary of CoMSIA results.

S.No.	CoMSIA Field	q^2	r^2	SEE	F	N	S.No.	CoMSIA Field	q^2	r^2	SEE	F	N
01	S/E/H/D/A	0.759	0.961	0.105	109.40	06	07	S/E/H	0.523	0.848	0.155	79.47	06
02	S/E/H/D	0.628	0.843	0.126	51.48	05	08	S/E/D	0.551	0.840	0.119	66.89	06
03	S/E/H/A	0.686	0.851	0.156	83.44	05	09	E/H/D	0.517	0.816	0.157	73.61	05
04	S/H/D/A	0.672	0.881	0.159	61.50	05	10	E/H/A	0.579	0.871	0.171	69.22	05
05	S/E/D/A	0.665	0.889	0.161	57.58	06	11	S/H/D	0.621	0.844	0.167	81.49	05
06	E/H/D/A	0.650	0.821	0.121	59.26	06	12	S/H/A	0.626	0.841	0.152	61.14	05

S, Steric field; E, Electrostatic field; H, Hydrophobic field; D, Donor field; A, Acceptor field; q^2, LOO cross-validated correlation coefficient; r^2, non-cross-validated correlation coefficient; N, number of components used in the PLS analysis; SEE: standard error of estimate; F value, F-statistic for the analysis.

Table 3: Summary of CoMFA and CoMSIA models.

Components	CoMFA	CoMSIA	Components	CoMFA	CoMSIA
q^2	0.742	0.759	Steric	0.703	0.225
r^2	0.923	0.961	Electrostatic	0.297	0.179
r^2_{pred}	0.901	0.900	Hydrophobic	-	0.201
F value	36.36	118.40	Donor	-	0.173
SEE	0.154	0.105	Acceptor	-	0.222

q^2, LOO cross-validated correlation coefficient; r^2, non-cross-validated coefficient of determination; r^2_{pred}, non-cross-validated correlation coefficient; N, number of components used in the PLS analysis; SEE, standard error of estimate; F value, F-statistic for the analysis.

Table 4: Experimental and predicted pIC_{50} values of training and test set.

Comp.	Experimental	COMFA Predicted	Residual	COMSIA Predicted	Residual	Comp.	Experimental	COMFA Predicted	Residual	COMSIA Predicted	Residual
1	4.283	4.238	0.045	4.222	0.061	22*	4.427	4.637	-0.21	4.397	0.030
2	4.346	4.171	0.175	4.364	-0.018	23*	3.205	3.163	0.042	3.197	0.008
3*	4.102	4.163	-0.061	4.154	-0.052	24	3.231	3.303	-0.072	3.329	-0.098
4	3.815	3.795	0.020	3.755	0.060	25	3.312	3.34	-0.028	3.29	0.022
5*	3.193	3.415	-0.222	3.300	-0.107	26	3.303	3.333	-0.03	3.377	-0.074
6	3.204	2.955	0.249	2.954	0.250	27	3.434	3.524	-0.09	3.506	-0.072
7	5.619	5.623	-0.004	5.666	-0.047	28	4.528	4.538	-0.01	4.396	0.132
8	3.869	3.741	0.128	3.741	0.128	29	4.190	4.145	0.045	4.106	0.084
9*	4.086	4.122	-0.036	4.051	0.035	30*	4.416	4.449	-0.033	4.337	0.079
10	3.095	3.200	-0.105	3.193	-0.098	31	3.908	3.774	0.134	3.775	0.133
11*	3.136	3.180	-0.044	3.172	-0.036	32*	4.008	4.064	-0.056	4.053	-0.045
12	4.812	4.676	0.136	4.654	0.158	33	4.053	3.973	0.08	4.028	0.025

13*	4.772	4.880	-0.108	4.836	-0.064	34	4.767	4.749	0.018	4.771	-0.004
14*	4.563	4.478	0.085	4.547	0.016	35	4.642	4.604	0.038	4.616	0.026
15	4.422	4.576	-0.154	4.430	-0.008	36	4.712	4.648	0.064	4.687	0.025
16*	4.764	4.800	-0.036	4.908	-0.144	37	3.167	3.279	-0.112	3.215	-0.048
17*	4.427	4.407	0.02	4.436	-0.009	38	3.16	3.208	-0.048	3.132	0.028
18	4.063	4.131	-0.068	4.185	-0.122	39	3.312	3.386	-0.074	3.413	-0.101
19	4.562	4.602	-0.04	4.428	0.134	40	3.283	3.393	-0.11	3.199	0.084
20*	4.531	4.503	0.028	4.601	-0.070	41	3.366	3.468	-0.102	3.43	-0.064
21*	4.463	4.517	-0.054	4.501	-0.038						

*Test Set Compounds

(a)   (b)
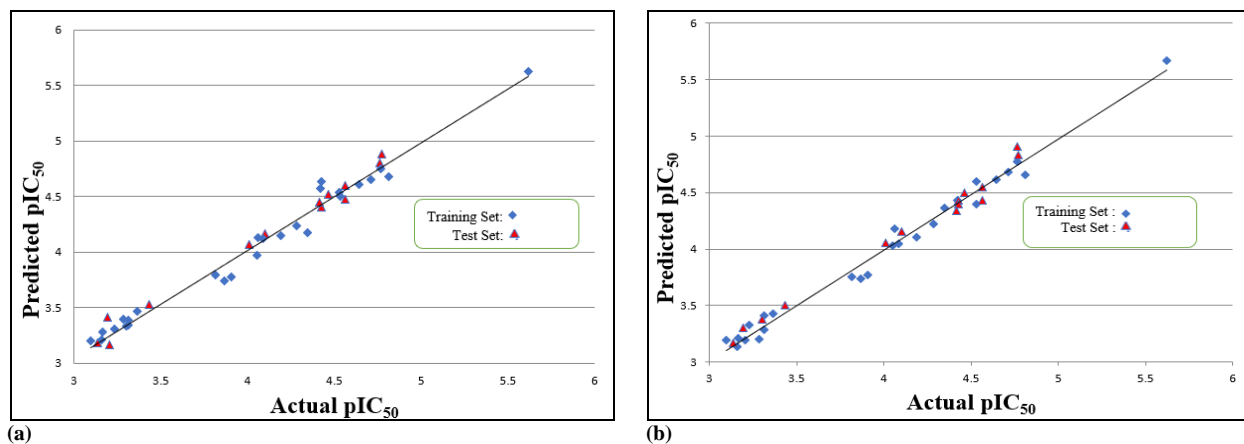
Figure 2: Graph of predicted versus actual pIC_{50} values from analyses for the training and test set compounds. (a) CoMFA (b) CoMSIA

DISCUSSION:
CoMFA contour map analyses:
In CoMFA steric contour map of most active compound 07(figure 3a), sterically favored regions are denoted by the green contour while the yellow contour represented sterically disfavoured region. However, in the electrostatic contour map, the blue contour indicates electron donating group favored areas and electron withdrawing group favored regions are designated by the red contour. In the CoMFA steric map, there is a large green contour covering the ring A, B and C showed the suitability of all the three rings for the antidiabetic activity. The green color contour around ring A and C indicates that the substitution of bulky group in this region is favorable for antidiabetic activity. In the CoMFA electrostatic map (figure 3b), blue contours appeared in the vicinity of ring A and C implies that the presence of electron donating group around ring A and C favors the antidiabetic activity.
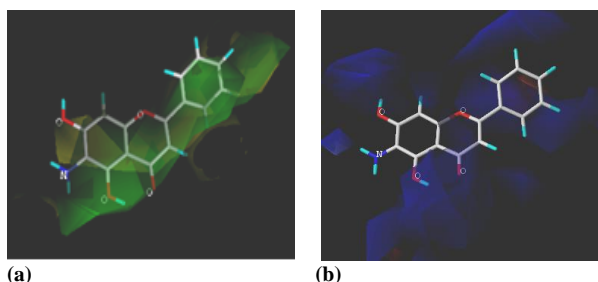

(a)   (b)

Figure 3: CoMFA STDEV* COEFF contour maps. (a) Steric fields (b)Electrostatic fields

CoMSIA contour map analyses:
The CoMSIA steric contour map is showed in figure 4(a). Green contours of the CoMSIA steric map around ring A, B and C can be well matched with the CoMFA steric contour map (figure 3a). In the same way, the CoMSIA electrostatic contour map (Figure 4b) is almost similar to the CoMFA electrostatic contour map (figure 3b). The CoMSIA steric and electrostatic contour maps are comparable to those of CoMFA, hence only the hydrophobic interaction and hydrogen-bond fields are described as follows. In the hydrophobic contour map (figure 4c), yellow contours specify the area where hydrophobic substituent can improve antidiabetic activity. The presence of yellow contours behind the ring A and B showed its suitability for antidiabetic activity. The yellow contours around the ring B also implies that the substitution of hydrophobic group at ring B can improve antidiabetic activity. However, white contour in the upper and lower side of hydrophilic ring C suggested that presence of ring C is also important for the antidiabetic activity. The presence of white contours near to R_3 and R_4 position in compound 07 suggested that hydrophilic groups at this position is favorable for antidiabetic activity. In the hydrogen-bond donor contour map (figure 5a), cyan contours appeared near to R_3 and R_4 position of ring A stipulated that substitution of hydrogen bond donor group at R_3 and R_4 position is favorable for antidiabetic activity of the compound. The presence of cyan contour in the neighborhood of ring B denoted that the substitution of hydrogen bond donor group at ring B may improve the biological activity of

the compound. whereas in the hydrogen bond acceptor map (Figure 5b), one magenta contour appeared near to oxo group of ring C, suggested that hydrogen bond

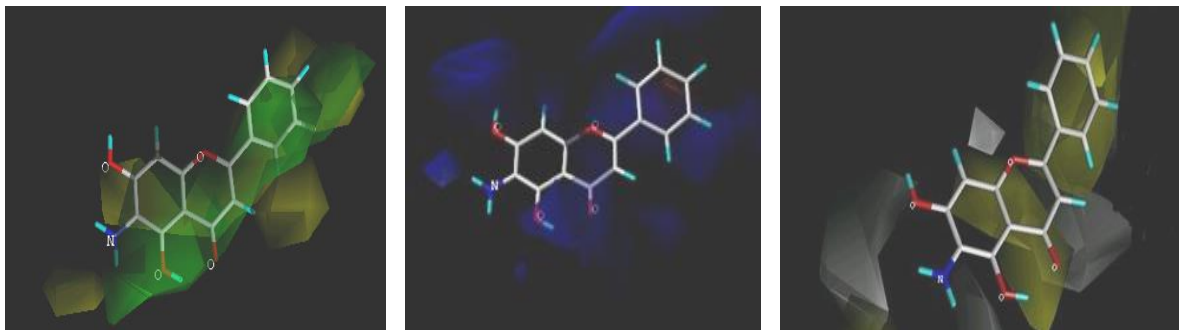acceptor oxo group at this position favors antidiabetic activity.

Figure 5: CoMSIA STDEV* COEFF contour maps. (a) Steric fields.(b) Electrostatic fields.(c) Hydrophobic fields

A big magenta contour developed in the vicinity of ring B denoted that substitution of hydrogen bond acceptor group on ring B may improve antidiabetic activity of the compounds. It signifies that at ring B substitution of both a hydrogen bond donor as well as hydrogen bond acceptor group is favorable for the enhancement of antidiabetic activity of compounds.

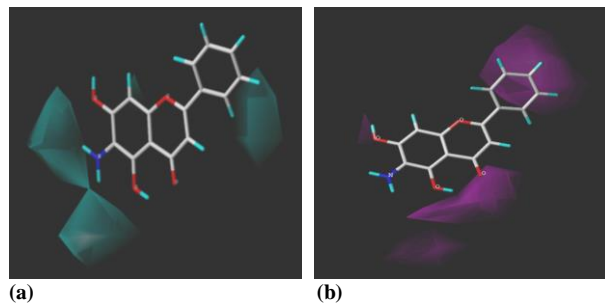**(a)**   **(b)**

Figure 6: (a) H-bond donor contour map: cyan contour indicates regions where hydrogen-bond donor groups increase activity. (b) H-bond acceptor contour map: magenta contour indicates regions where hydrogen-bond acceptor groups increase activity

CONCLUSION:
In summary, we have effectively utilized CoMFA and CoMSIA techniques to develop very predictive 3D-QSAR models for forty-one structurally diverse flavone derivatives. The good relationship between experimental and predicted activity for test and training set compounds ascertained the reliability of these QSAR models. In this research work, the QSAR models were also validated by internal LOO cross-validation methods and external test set methods. It is concluded that modifications in the structure of flavones according to the information obtained from 3D-QSAR analyses could lead to new flavones with effective antidiabetic activity. The results showed here may be considered useful when designing novel and potential antidiabetic agents.

CONFLICT OF INTEREST:
The authors have no conflicts of interest regarding this research work**.**

REFERENCES:
1. World Health Organisation, WHO 2020 World Diabetes Report. https://www.who.int/health-topics/diabetes
2. Verspohl EJ. Novel Pharmacological Approaches to the Treatment of Type 2 Diabetes. Pharmacological Reviews. 2012; 64(2): 2188-2237.
3. Chiba S. Molecular mechanism in alpha glucosidase and alpha amylase. Biosci. Biotechnol. Biochem. 199; 61(8): 1233-39.
4. Hsieh PC, Huang G, Ho Y, Lin Y, Huang S, Chiang Y, Tseng MC, Chang YS. Activities of antioxidants, α-Glucosidase inhibitors and aldose reductase inhibitors of the aqueous extracts of four *Flemingia* species in Taiwan. *Bot Stud.* 2010; 51: 293-302.
5. Ahmed N. Advanced glycation end products role in pathology of diabetic comlications. Diab. Res. Clin. Pr. 2005; 67(1): 3-21.
6. Asano N. Glycosidase inhibitors: update and perspectives on practical use. Glycobiology 2003; 13(10): 93-104.
7. Chougale AD, Ghadyale VA, Panaskar SN, Arvindekar AU. Alpha glucosidase inhibition by stem extract of Tinospora cordifolia. J. Enzyme Inhib. Med. Chem. 2009; 24(4): 998-1001.
8. Kashtoh H, Hussain S, Khan A, Saad SM, Khan AJ, Khan KM, Perveen S, Choudhary M I. Oxadiazoles and thiadiazoles: Novel a-glucosidase inhibitors. Bioorg and Med Chem. 2014; 22(19): 5454-65.
9. Kumar S, Narwal S, Kumar V, Prakash O. α-glucosidase inhibitors from plants: A natural ap α-glucosidase inhibitors from plants: A natural approach to treat diabetes. Pharmacogn Rev. 2011; 5(9): 19–29.
10. Singh M, Kaur M, Silakari O. Flavones: An important scaffold for medicinal chemistry. Eur J Med Chem. 2014; 84: 206-239.
11. Xu JD, Zhang LW, Liu YF. Synthesis and antioxidant activities of flavonoids derivatives, troxerutin and 30,40,7-triacetoxyethoxyquercetin Chin. Chem. Lett. 2013; 24(3):223-226.
12. Zhengn JB, Zhang HF, Gao H. Investigation on electrochemical behavior and scavenging superoxide anion ability of chrysin at mercury electrode topon. J. Chem. 2005; 23(8): 1042-1046.
13. Prasada Rao K., Santha Kumari K., Mohan S. Synthesis, Characterization and Antimicrobial activity of Some Flavones. Asian J. Research Chem. 2013; 6(2): 163-165.
14. Shanmugapriya E, Ravichandiran V, Vijey Aainandhi M. Molecular docking studies on naturally occurring selected flavones against protease enzyme of Dengue virus. Research J. Pharm. and Tech. 2016; 9(7): 929-932.
15. Kumar L, Verma R. Molecular docking-based approach for the design of Novel Flavone Analogues as inhibitor of Beta-

Hydroxyacyl-ACP Dehydratase HadAB complex. Research J. Pharm. and Tech. 2017; 10(8): 2439-2445.

16. Gejalakshmi S, Harikrishnan N, Mohameid AS. In-Vitro and In-Silico Alpha Glucucosidase Inhibitory activity of Oroxylum indicum. Research Journal of Pharmacognosy and Phytochemistry. 2021; 13(3): 119-5.

17. Hanhineva K, Torronen R, Bondia-Pons I, Pekkinen J, Kolehmainen M, Mykkanen H, Poutanen K. Impact of dietary polyphenols on carbohydrate metabolism. Int. J. Mol. Sci. 2010; 11(4): 1365-1402.

18. Sainy J, Sharma R. QSAR analysis of thiolactone derivatives using HQSAR, CoMFA and CoMSIA, SAR QSAR Enviro. Res. 2015; 26(10): 873–892.

19. Mandloi N, Sharma R, Sainy J, Patil S. Exploring Structural Requirement for Design and Development of compounds with Antimalarial Activity via CoMFA, CoMSIA and HQSAR. Research J. Pharm. and Tech. 2018; 11(8): 3341-3349.

20. Pai A, B. Jayashree S. Computational Approach for the Design of Flavone based CDK2/CyclinA Inhibitors: A Simulation Study Employing Pharmacophore based 3D QSAR. Research J. Pharm. and Tech. 2019; 12(5): 2299-2303.

21. Karthikeyan L, Hari BB, Rajasekaran A, Arivukkarasu R. Molecular Docking Studies of Flavones in Gentianaceae Family against Liver Corrective Targets. Res. J. Pharmacognosy and Phytochem. 2019; 11(2): 49-53.

22. Tanveer H, Raza MG, Sayed H M, Singh PK, Baqri SSR. Normal Mode Analysis, Electronic Parameters and molecular docking study of 3, 5, 4'-Trihydroxy-6, 7-Dimethoxy-Flavone (Eupalitin) using First Principle. Asian J. Research Chem. 2017; 10(6): 789-797.

23. Bhavanisha Rithiga S, Shanmugasundaram S. Virtual Screening of Pentahydroxyflavone – A Potent COVID-19 Major Protease Inhibitor. Asian J. Res. Pharm.Sci. 2021; 11(1): 7-14.

24. Kumawat D, Goswami R, Pathak S, Gupta DK, Dwivedi S K, Chaturvedi SC. Molecular Modeling Study of Some β-Ketoacyl-acyl Carrier Protein Synthase III Inhibitors as Antibacterial Agents. Asian J. Res. Pharm. Sci. 2019; 9(4): 253-259.

25. Stewart JJP. Optimization of parameters for semiempirical methods I. Method. J. Comput. Chem. 1989; 10(2): 209–220.

26. Cramer III RD, Patterson DE, Bunce JD. Comparative molecular field analysis (CoMFA): I. Effect of shape on binding of steroids to carrier proteins. J. Am. Chem. Soc. 1988; 110(18): 5959–5967.

27. Klebe G, Abraham U, MietzneT. Molecular similarity indexes in a comparative-analysis (CoMSIA) of drug molecules to correlate and predict their biological activity. J. Med. Chem. 1994; 37(24): 4130–4146.

28. SYBYL-X 2.1, Tripos Inc., St. Louis, MO.

29. Moda TL, Montanarib CA, Andricopulo AD. Hologram QSAR model for the prediction of human oral bioavailability. Bioorg. Med. Chem. 2007; 15(24): 7738–7745.

30. Hong Gao and Jun Kawabata α-Glucosidase inhibition of 6-hydroxyflavones. Part 3: Synthesis and evaluation of 2,3,4-trihydroxybenzoyl-containing flavonoid analogs and 6-aminoflavones as a-glucosidse inhibitors.bmcl. 2005; 13(5): 1661-1671.

31. Imran S, Taha Muhammad, Ismail Nor Hadiani, Kashif Syed Muhammad C, Rahim Fazal D, Jamil Waqas C, Hariono Maywan E, Yusuf Muhammad E, Wahab Habibah. Synthesis of novel flavone hydrazones: In-vitro evaluation of α-glucosidase inhibition, QSAR analysis and docking studies. EJMC 105(2015): 156-170.

32. Cho S.J. and Tropsha A. Cross-validated R2-guided region selection for comparative molecular field analysis: A simple method to achieve consistent results. J. Med. Chem. 1995; 38(7): 1060–1066.

33. Tong W, Lowis DR, Perkins R, Chen Y, Welsh WJ, Goddette DW, Heritage TW, and Sheehan DM. Evaluation of quantitative structure–activity relationship methods for large-scale prediction of chemicals binding to the estrogen receptor. J. Chem. Inf. Comput. Sci. 38. 1998; 22(8): 669–677.

34. Waller CL. A comparative QSAR study using CoMFA, HQSAR, and FRED/SKEYS paradigms for estrogen receptor binding affinities of structurally diverse compounds. J. Chem. Inf. Compu.t Sci. 2004; 44(2): 758–765.

35. Clark M, Cramer III RD, Opdenbosch NV. Validation of the general purpose Tripos 5.2 forcefield. J. Comput. Chem. 1989; 10(8): 982–1012.

36. Dunn WJ, Wold S, Edlund V, Hellherg S, and Gasteiger J. Multivariate structure-activity relationships between data from a battery of biological tests and an ensemble of chemical descriptors: The PLS method, Quant. Struct.-Act. Relat. 1984; 3: 131–137.

37. Wold S, Sjöström M, and Eriksson L. PLS-regression: A basic tool of chemometrics, Chemom. Intell. Lab. Syst. 2001; 58(2): 109–130.

38. Cramer R.D. Partial least squares (PLS): Its strengths and limitations. Perspect Drug Discov. Des.1. 1993; 1(2): 269–278.

39. S. Wold and L. Ericksson, Partial least squares projections to latent structures (PLS) in chemistry, In Encyclopedia of Computational Chemistry, Ragu and P. Schleyer, eds., John Wiley and Sons, Chichester, 1998, pp. 2006–2021.

40. A.K. Debnath, Combinatorial library design and evaluation, in Principles, Software, Tools and Application in Drug Discovery, K. Ghose and V.N. Viswanadhan, eds., Marcel Dekker Inc, New York, NY, 2001; pp. 73–129.

41. Walker JD, Jaworska J, Comber MH, Schultz TW, Dearden JC. Guidelines for developing and using quantitative structure-activity relationships. Environ Toxicol. Chem. 2003; 22(8): 1653–1665.